

Role of cohesion in the material description of biofilms

I. Klapper and J. Dockery

Department of Mathematical Sciences and Center for Biofilm Engineering, Montana State University, Bozeman, Montana 59717, USA

(Received 6 January 2006; revised manuscript received 15 March 2006; published 5 September 2006)

Biofilm structure plays an important role in biofilm function and control. It is thus important to determine the extent to which mechanics may determine structure in biofilms. We consider a generic qualitative constitutive description of biofilm incorporating as assumptions a small number of fundamental physical properties of biofilm viscoelasticity and cohesion. Implications of cohesive energy on biofilm structure are then explored. Steady solutions and energy minima are studied and it is demonstrated that cohesion energy leads naturally to a free surface film state. It is found that in many circumstances, biofilms could be subject to heterogeneity formation via spinodal decomposition. Such material heterogeneity may have important implications for structural stability in biofilms both on short and long time scales.

DOI: [10.1103/PhysRevE.74.031902](https://doi.org/10.1103/PhysRevE.74.031902)

PACS number(s): 87.15.La, 87.16.Ac, 64.75.+g, 82.70.-y

I. INTRODUCTION

Microorganisms commonly aggregate in the form of a biofilm, a structure in which they encase themselves within a matrix of extracellular polymers. This architecture has proven an extremely effective survival strategy and can be found in virtually any wet or damp environment. In fact most bacteria are believed to live in such communities. As such, they inevitably become a subject of interest in numerous contexts. Biofilms are ubiquitous in systems arising in industry, medicine, water distribution and treatment, etc. They are certainly ever present domestically in water pipes, kitchens, air ducts, hot tubs, etc. In short, biofilms are unavoidably an essential component of our environment. This is especially significant as bacteria within biofilms are equipped with extra protection from disinfection or removal due to their polymeric encasement through a number of different mechanisms. For an overview of biofilm processes see Ref. [1].

Yet the basic physical properties of biofilms are not well understood. Internal structure and mechanics have proven nontrivial [2]. This paper seeks to address one important question for understanding biofilm mechanics, namely, on a phenomenological level what holds a biofilm together and how does a biofilm respond to long time-scale stress? On the one hand, internal cohesiveness must play a role in failure, i.e., sloughing, in response to short-term stress. On the other hand, while biological factors (e.g., growth and decay) may be dominant over the long term, the effects of cohesion can be expected to be influential as well. It is thus important to have a physical framework in place. We propose here a description of the inherent “stickiness” of biofilms through the introduction of a cohesion energy and its resulting stress.

There is a relatively large body of work on biofilm modeling focusing principally on growth processes, e.g., Ref. [3]. The literature on mechanical properties and modeling is more sparse. Notably, Ref. [4] considered a microscale model of biofilm formation, and Ref. [5] regarded biofilms as solids for the purpose of modeling detachment. Recent experimental work suggests that biofilms behave as viscoelastic fluids, e.g., Ref. [6]. We include growth and viscoelastic stress response here for completeness but focus on cohesive effects. With regards to cohesion, Ref. [7] modeled biofilm

as a gel and introduced a two phase description and an osmotic pressure. Such a description is useful if one wishes to study matrix density variations within a biofilm (which as a whole is mostly water and hence incompressible) and we adopt that practice here. A multiphase formulation was also developed in Ref. [8] but with the purposes of studying multispecies interaction effects, not mechanics. A related two phase description in a biological application was proposed in Ref. [9]. Also recent tumor model studies, an area with some similarity to biofilm modeling, have begun using two-phase descriptions, e.g., Ref. [10].

In this paper we first introduce a two-phase system of conservation and constitutive laws for a viscoelastic cohesive system (Sec. II). The derivation is based on a model developed for polymer-solvent theory. A short discussion of the mean field cohesion assumptions is given in Sec. III. Analysis and computations of one-dimensional systems with cohesion effects are presented in Sec. IV.

II. TWO-PHASE BIOFILM EQUATIONS

A. General equations

We follow and adapt two-phase polymer-solvent theory [11]. Let $\phi_b(\mathbf{x}, t)$, $\rho_b(\mathbf{x}, t)$, $\mathbf{u}_b(\mathbf{x}, t)$ be the biomaterial volume fraction, density, and velocity at position \mathbf{x} and time t , and let $\phi_s(\mathbf{x}, t)$, $\rho_s(\mathbf{x}, t)$, $\mathbf{u}_s(\mathbf{x}, t)$ be the solvent volume fraction, density, and velocity at position \mathbf{x} and time t . Here ρ_b and ρ_s are densities with respect to their corresponding volume fractions ϕ_b and ϕ_s . Note that ϕ_b and ϕ_s are related by $\phi_b + \phi_s = 1$. We assume that ρ_b and ρ_s are in fact constants, i.e., ρ_b and ρ_s are independent of \mathbf{x} and t . Then we have the mass transport relations

$$\begin{aligned} \frac{\partial \phi_b}{\partial t} + \nabla \cdot (\phi_b \mathbf{u}_b) &= \frac{G}{\rho_b}, \\ \frac{\partial \phi_s}{\partial t} + \nabla \cdot (\phi_s \mathbf{u}_s) &= -\frac{G}{\rho_s}, \end{aligned} \quad (1)$$

where G is a growth source term (neglected in the following). Using $\phi_s = 1 - \phi_b$, the second of these equations can be

eliminated. Summing these equations results in the incompressibility condition $\nabla \cdot \mathbf{u} = 0$ where $\mathbf{u} = \phi_b \mathbf{u}_b + (1 - \phi_b) \mathbf{u}_s$.

The momentum conservation equations are

$$\begin{aligned} \rho_b \frac{\partial}{\partial t} (\phi_b \mathbf{u}_b) + \rho_b \nabla \cdot (\phi_b \mathbf{u}_b \otimes \mathbf{u}_b) \\ = \phi_b \nabla \cdot \Pi^{(c)} + \nabla \cdot \Pi^{(b)} - \zeta (\mathbf{u}_b - \mathbf{u}_s) + \phi_b \nabla p, \\ \rho_s \frac{\partial}{\partial t} (\phi_s \mathbf{u}_s) + \rho_s \nabla \cdot (\phi_s \mathbf{u}_s \otimes \mathbf{u}_s) \\ = \nabla \cdot \Pi^{(s)} + \zeta (\mathbf{u}_b - \mathbf{u}_s) + (1 - \phi_b) \nabla p, \end{aligned} \quad (2)$$

where $\Pi^{(c)}$, $\Pi^{(b)}$, $\Pi^{(s)}$ are stress tensors to be described below, p is a hydrostatic pressure determined by the incompressibility requirement $\nabla \cdot \mathbf{u} = 0$, and $\zeta = \zeta(\phi_b)$ is a drag coefficient. We assume that $\zeta(\phi_b) = \zeta_0 \phi_b (1 - \phi_b)$ for some constant ζ_0 (with Stokes' drag as intuition). Thus $\zeta(\mathbf{u}_b - \mathbf{u}_s)$ provides a frictional coupling between the two phases. Equations (2) simplify after noting that biofilms are highly viscous [12] and hence the left-hand-side inertial terms can generally be neglected. We shall do so here.

The solvent stress tensor $\Pi^{(s)}$ is the Navier-Stokes shear stress and the biomaterial stress tensor $\Pi^{(b)}$ is the viscoelastic stress resulting from biofilm deformation [6]. $\Pi^{(c)}$ arises from the presence of a cohesion energy of the form

$$E = \int \left(f(\phi_b) + \frac{\kappa}{2} |\nabla \phi_b|^2 \right) dV, \quad (3)$$

where $f(\phi_b)$ is a homogeneous mixing energy density and $(\kappa/2)(\nabla \phi_b)^2$ penalizes spatial inhomogeneity. (We discuss the form of f in Sec. III.) E is sometimes called a chemical energy of mixing.

Long-time effects of E on biofilm structure are the main focus of this paper. Using the equation $\dot{\phi}_b + \nabla \cdot (\phi_b \mathbf{u}_b) = 0$ and requiring on solid boundaries that $\nabla \phi_b \cdot \mathbf{n} = 0$, $\mathbf{u}_b = 0$, and that on free boundaries $\phi_b = 0$,

$$\begin{aligned} \frac{d}{dt} E &= \int [f'(\phi_b) - \kappa \nabla^2 \phi_b] \dot{\phi}_b dV \\ &= - \int [f'(\phi_b) - \kappa \nabla^2 \phi_b] [\nabla \cdot (\phi_b \mathbf{u}_b)] dV \\ &= - \int (\phi_b \nabla \cdot \Pi^{(c)}) \cdot \mathbf{u}_b dV, \end{aligned} \quad (4)$$

where

$$\Pi^{(c)} = - [f'(\phi_b) - \kappa \nabla^2 \phi] \mathbf{I}.$$

Equation (4) is in the form of a work integral $\dot{E} = \int \mathbf{f} \cdot \mathbf{u}_b dV$ and hence for purposes of momentum conservation we include the forcing term $\phi_b \nabla \cdot \Pi^{(c)}$ in the biomaterial momentum equation. Alternatively, the same result may be obtained by taking the appropriate functional derivative of E with respect to the allowable velocities \mathbf{u}_b .

B. Biomaterial equation

Neglecting inertial terms in (2) and eliminating the pressure, we obtain after some algebra (as in Ref. [11])

$$\begin{aligned} \mathbf{u}_b - \mathbf{u}_s &= \zeta^{-1} [\phi_b (1 - \phi_b) \nabla \cdot \Pi^{(c)} + (1 - \phi_b) \nabla \cdot \Pi^{(b)} \\ &\quad - \phi_b \nabla \cdot \Pi^{(s)}] \end{aligned} \quad (5)$$

and then by using (1) (again with $G=0$),

$$\begin{aligned} \frac{\partial \phi_b}{\partial t} + \nabla \cdot (\phi_b \mathbf{u}) &= - \nabla \cdot [\phi_b (1 - \phi_b) (\mathbf{u}_b - \mathbf{u}_s)] \\ &= \zeta_0^{-1} \nabla \cdot [\phi_b (1 - \phi_b) f''(\phi_b) \nabla \phi_b] \\ &\quad - \zeta_0^{-1} \kappa \nabla \cdot [\phi_b (1 - \phi_b) \nabla \nabla^2 \phi_b] \\ &\quad - \zeta_0^{-1} \nabla \cdot [(1 - \phi_b) \nabla \cdot \Pi^{(b)}] \\ &\quad + \zeta_0^{-1} \nabla \cdot (\phi_b \nabla \cdot \Pi^{(s)}). \end{aligned} \quad (6)$$

Equation (6) has similarities to the Cahn-Hilliard equation [13]. In particular, neglecting those terms explicitly dependent on deformation stress, we obtain

$$\frac{D \phi_b}{Dt} = \nabla \cdot [a(\phi_b) f''(\phi_b) \nabla \phi_b] - \kappa \nabla \cdot [a(\phi_b) \nabla \nabla^2 \phi_b], \quad (7)$$

where $a(\phi_b) = \zeta_0^{-1} \phi_b (1 - \phi_b)$. Note that the effective diffusivity $a(\phi_b) f''(\phi_b)$ is negative at spatial locations such that $f''(\phi_b) < 0$, suggesting the possibility of instability. While (7) is a degenerate parabolic equation without a maximum principle, one can show that if $0 \leq \phi_b(t, x) \leq 1$ at $t=0$ then the same is true for all $t > 0$, see Ref. [14]. This type of equation also arises in the study of thin films, see e.g., Ref. [15] and the references therein. We stress however that ϕ_b is a volume fraction, not a film height, and that no thin film approximation is made in this paper.

We will concentrate attention on Eq. (7) in the remaining sections of the paper. To justify neglect of the elastic component of $\Pi^{(b)}$, we are assuming evolution time scales longer than the elastic relaxation time (approximately 20 minutes, see Ref. [12]). To justify neglect of viscous stresses in $\Pi^{(b)}$ and $\Pi^{(s)}$, we are assuming slow rates of deformation within the biofilm.

An evolution equation for the cohesion energy is obtained by taking the inner products of Eqs. (2) with \mathbf{u}_b and \mathbf{u}_s , respectively. Using $\nabla \cdot \mathbf{u} = 0$ and neglecting G as well as the inertial terms, we obtain

$$\frac{dE}{dt} = - \int \nu_s (\nabla \mathbf{u}_s)^2 dV - \int \nu_b (\nabla \mathbf{u}_b)^2 dV - \int \zeta (\mathbf{u}_b - \mathbf{u}_s)^2 dV. \quad (8)$$

(If inertial terms are included then time derivatives of the kinetic energies of the two phases appear on the left-hand side.) The parameters ν_s , ν_b , ζ vary as a function of $\phi_b(\mathbf{x})$ but all are positive for $0 < \phi_b < 1$. We assume in (8) that deformations occur on a sufficiently slow time scale so that the stress tensor $\Pi^{(b)}$ can be regarded as that of a Newtonian viscous fluid and also require that velocities or viscous

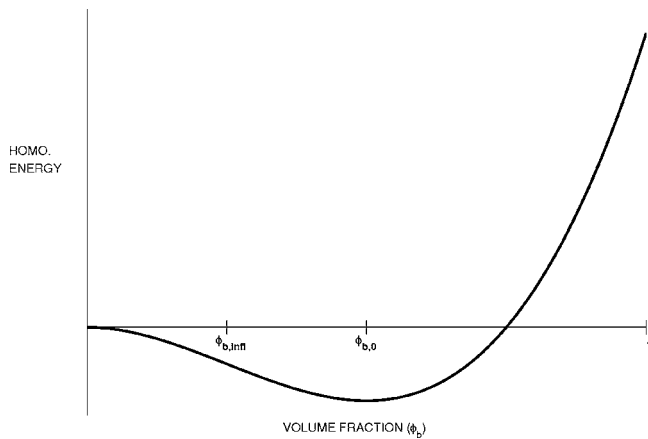


FIG. 1. Form of the homogeneous part $f(\phi_b)$ of the cohesion energy density.

stresses are zero on boundaries. Under these conditions (8) indicates decay of the energy E in time.

III. THE FUNCTION $f(\phi_b)$

A few basic assumptions are made concerning f , the homogeneous part of the cohesion energy density, see Fig. 1. The first is that biofilm material is sticky, meaning in particular that $f(\phi_b)$ has a nonzero minimum at some value $\phi_{b,0}$ of the volume fraction. For ϕ_b larger than $\phi_{b,0}$ we expect f to increase (biofilm prefers presence of some solvent) and for ϕ_b smaller than $\phi_{b,0}$ we expect f to increase and approach 0. A second assumption is that f has an inflection point $\phi_{b,\text{inf}}$ with $0 < \phi_{b,\text{inf}} < \phi_{b,0}$. [This will be true if, for example, f decays faster than linearly as $\phi_b \rightarrow 0$. Such will generally be the case: volume fraction ϕ_b is proportional to r^{-3} where r is the length scale of local separation of biofilm elements. Likewise, the local energy density $f(\phi_b)$ is proportional to $r^{-3}V(r)$ for some potential function $V(r)$. As it can be expected that $V(r) \rightarrow 0$ as $r \rightarrow \infty$, then we can thus expect $f(\phi_b)/\phi_b \rightarrow 0$ as $\phi_b \rightarrow 0$.] Finally, in addition we assume $f'(\phi_b)$ is convex for simplicity only. As a consequence f has only one inflection point.

There is at present not a great deal of data available with which to quantitatively estimate the form of f (or of E), though some preliminary data regarding biofilm energy storage exists, see, e.g., Ref. [16]. In any case, the precise form of material descriptions can be expected to vary from biofilm to biofilm. However we are more interested in qualitative observations here so we do not address this concern at the current time.

IV. TIME INDEPENDENT SOLUTIONS IN 1D

A. Equations

The derived equations simplify appreciably for slow motions in one dimension. First, the condition $\nabla \cdot \mathbf{u} = \partial_x u = 0$ requires in 1D that u is constant in space. By Galilean invariance we may assume that $u(x, t) = 0$. Also, the stress tensors $\Pi^{(b)}$ (for slow deformations) and $\Pi^{(s)}$ can be neglected be-

cause they contain only compressive terms which are assumed small—we are effectively assuming deformations such that the induced cohesion force is large compared to the effects of compressional stress. Then, using $u = \phi_b u_b + (1 - \phi_b) u_s = 0$ with (5) and (7), we obtain the system

$$\begin{aligned} \frac{\partial \phi_b}{\partial t} &= - \frac{\partial}{\partial x} \left(a(\phi_b) \frac{\partial \pi^{(c)}}{\partial x} \right), \\ u_b &= - \frac{1 - \phi_b}{\zeta_0} \frac{\partial \pi^{(c)}}{\partial x}, \\ u_s &= \frac{\phi_b}{\zeta_0} \frac{\partial \pi^{(c)}}{\partial x}, \end{aligned} \quad (9)$$

where $\pi^{(c)} = -f'(\phi_b) + \kappa \phi_{b,xx}$. Note that ϕ_b decouples from u_b and u_s .

Steady solutions of (9) (or the original multidimensional system) satisfy $\phi_b \nabla \cdot \Pi^{(c)} = 0$, $\mathbf{u}_b = \mathbf{u}_s = \mathbf{u} = 0$, i.e., $u_b = u_s = u = \phi_b \partial \pi^{(c)} / \partial x = 0$ in 1D. Using (8) and (2) it is seen that such solutions are linearly stable if and only if they are local minima (constrained to the surface of solutions with the same given total mass) of the cohesion energy E .

We consider the possibility of steady solutions with spatially periodic ϕ_b as well as solutions that satisfy Neumann boundary conditions

$$\phi_x|_{x=0,L} = \phi_{xxx}|_{x=0,L} = 0$$

in finite one-dimensional domains. Any steady state must satisfy

$$-d\pi^{(c)}/dx = f''(\phi_b)\phi_{b,x} - \kappa\phi_{b,xxx} = A[a(\phi_b)]^{-1}$$

for some constant A . However it is easily seen that under periodic boundary conditions (by integrating over a period) or Neumann boundary conditions (by checking at either endpoint), A must be zero. In some instances we will consider weak solutions; in these cases $A=0$ is forced as a jump condition. Thus we require that $0 = f''(\phi_b)\phi_{b,x} - \kappa\phi_{b,xxx}$. Integrating once more we obtain

$$\pi^{(c)} = -f'(\phi_b) + \kappa\phi_{b,xx} = D \quad (10)$$

for some integration constant D . Note that

$$D = -L^{-1} \int_0^L f'(\phi_b) dx,$$

where $[0, L]$ is the domain of support for ϕ_b . Note also that D is independent of κ . Hence κ (or, more precisely, $\sqrt{\kappa}$) serves as a spatial scaling factor. These last statements hold for all solutions to be considered except those of type shown in Fig. 7, panel 4 (see below).

B. Phase plane analysis

Equation (10) can be written as the system

$$\dot{u} = v,$$

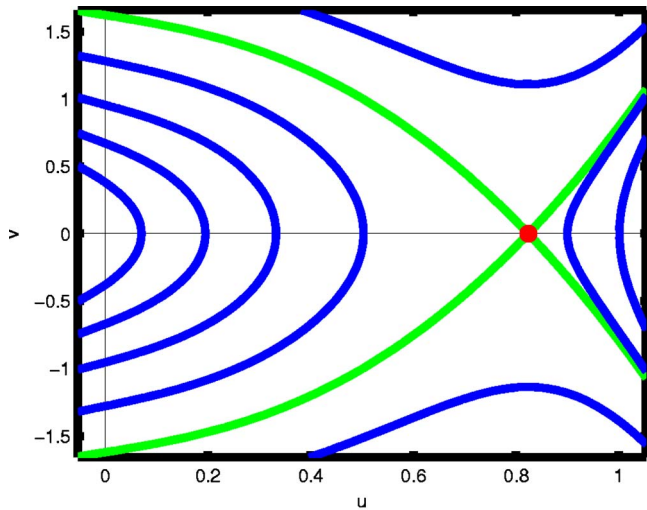


FIG. 2. (Color online) $D < 0$.

$$\dot{v} = -U'(u) \tag{11}$$

with $u = \phi_b$, $v = \phi_{b,x}$, and $U(u) = \kappa^{-1}[-f(u) - Du]$. Here the “time” derivatives of u and v , denoted by dots, correspond to spatial derivatives of ϕ_b . The primed derivative refers to differentiation with respect to u . In order that $0 \leq \phi_b \leq 1$, we consider only those solutions of (11) that satisfy $0 \leq u \leq 1$.

Representative phase planes for the system (11) are shown in Figs. 2–5 for different values of the parameter D . There are four possible types of spatially periodic steady-state solutions. These are depicted in Fig. 6. The two on the left-hand side extend smoothly to be L -periodic whereas the two on the right-hand side have less regularity and are called droplet steady states in the thin film literature. (Here ϕ_b replaces film height h , and droplet refers to localization of biomaterial rather than to a physical drop.) The third profile has zero contact angles at $\phi_b = 0$ whereas the fourth has non-zero contact angles. (For convenience we will continue to use the thin film jargon contact angle; the reader should be aware however that the angle to which we refer arises from

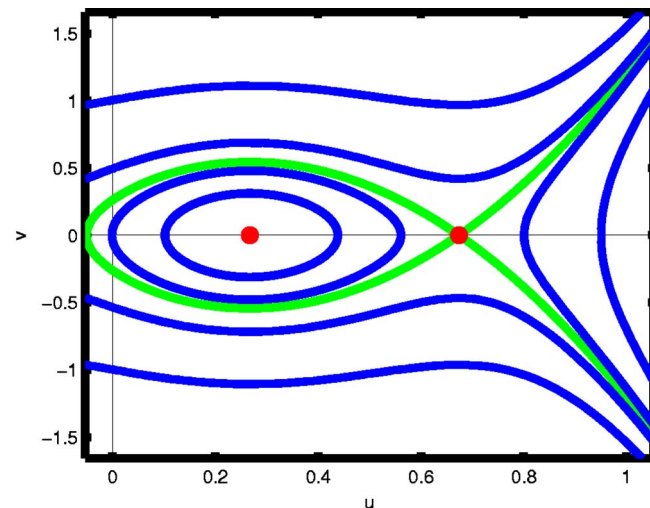


FIG. 3. (Color online) $0 < D < D^*$.

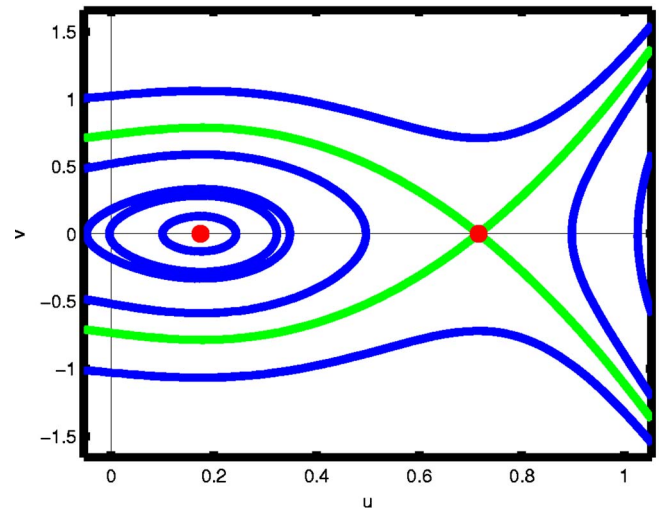


FIG. 4. (Color online) $D = D^*$.

contact with the $\phi_b = 0$ axis, see, e.g., Figs. 6 and 7, and not physical contact with a surface. We reiterate that ϕ_b is a volume fraction and not a film height.) Both have support within the interval $(0, L)$ and are apparent possible long-time limits of a L -periodic solution for the evolution equation (11) (see below). There are analogous classes of steady-state solutions which satisfy Neumann or no-flux boundary conditions. Monotone steady-state solutions of these types are depicted in Fig. 7.

As a remark, we note that a fifth class of steady-state solutions exist which could be called “inverse droplet” states. These reduced regularity solutions consist of regions with $\phi_b = 1$ interspersed between regions with $\phi_b < 1$ (much like inverted droplet solutions). However all such states are of higher energy than the corresponding constant volume fraction solutions with the same total biomaterial mass, and hence will not be further considered.

1. Spatially constant steady states

The simplest class of steady solutions are the constant solutions, $\phi_b \equiv C$. Note then that $D = -f'(C)$. The fixed points

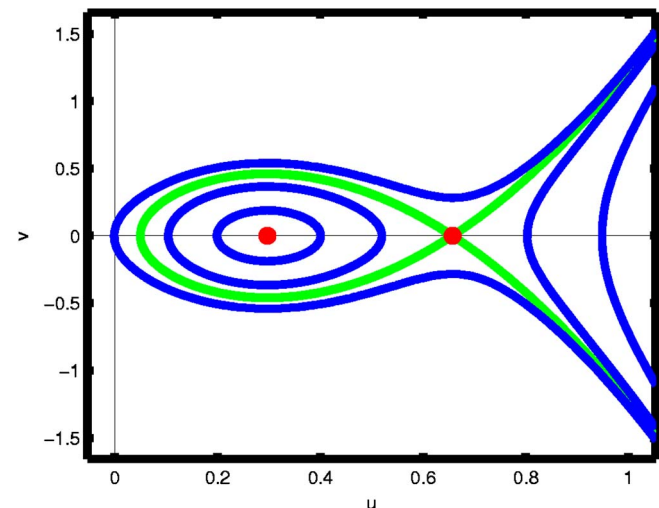


FIG. 5. (Color online) $D^* < D < D_{\max}$.

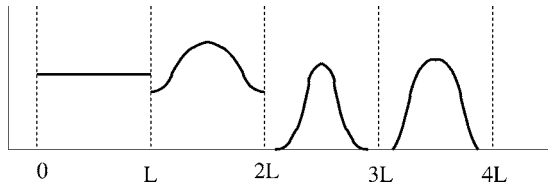


FIG. 6. Four types of periodic steady states.

in Figs. 2–5 correspond to these spatially constant steady-state solutions. In the case that $\phi_b > \phi_{b,0}$, i.e., volume fraction is larger than the minimum energy value, then $f'(\phi_b) > 0$ (see Fig. 1) so $D = -f'(C) < 0$ (Fig. 2) and we observe that there is a unique constant state for each value of ϕ_b . At $D=0$ there is a second trivial fixed point $u=v=0$ corresponding to $\phi_b=0$. Conversely, for $\phi_b < \phi_{b,0}$, steady states satisfy $f'(C) < 0$, i.e., $D > 0$. In this case there are two possible constant steady states $\phi_b \equiv C$ for each value of $D < D_{\max}$ (Figs. 3–5), one on each side of the inflection point $\phi_{b,\text{infl}}$. Here $D_{\max} = \max(-f') = -f'(\phi_{b,\text{infl}})$. At $D = D_{\max}$, the two fixed points coalesce and there is again a single corresponding spatially constant steady state. No physically relevant solutions exist for D larger than D_{\max} .

A straightforward analysis addresses linear stability of these constant solutions to spatially varying perturbations. For f as in Fig. 1, solutions are linearly stable for $C > \phi_{b,\text{infl}}$ and linearly unstable for $C < \phi_{b,\text{infl}}$. That is, low density (relative to $\phi_{b,\text{infl}}$) homogeneous biofilms are unstable to formation of “clumps” (the spinodal instability, see Ref. [17]) since total cohesion energy can be reduced by biofilm segregation at values of ϕ_b for which the graph of $f(\phi_b)$ is concave down. Constant solutions are linearly stable at volume fractions greater than $\phi_{b,\text{infl}}$ where $f(\phi_b)$ is concave up. However, it may still be the case for some values of $C > \phi_{b,\text{infl}}$ that $\phi_b \equiv C$ is linearly stable but nonlinearly unstable, i.e., unstable to large perturbations. This issue will be further addressed in the numerical results section.

2. Spatially nonconstant steady states

We consider first spatially periodic steady states $\phi_b(x)$. Such solutions correspond in Fig. 2–5 to either periodic orbits or to orbits that begin and end on the v axis (where $\phi_b = 0$). Solutions corresponding to these latter orbits can be pieced together with $\phi_b=0$ solutions to form periodic droplet solutions, e.g., Fig. 6, panels 3 and 4.

Also, we consider solutions $\phi_b(x)$ satisfying Neumann boundary conditions on a finite interval. In this case we must look for orbits in the phase portraits, Fig. 2–5, that begin and end on the u axis (where $\phi_{b,x} = 0$). In addition, orbits with

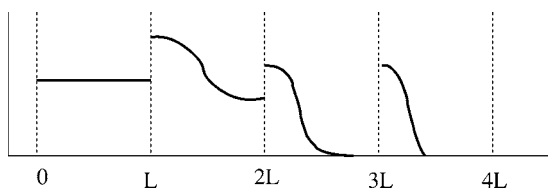


FIG. 7. Four types of monotone no-flux steady-state solutions.

beginning or ending points on the v axis are allowable—solutions corresponding to such orbits can be pieced together with $\phi_b=0$ solutions in such a way as to satisfy the boundary conditions.

Bifurcations in solution behavior occur at $D=0$, $D=D^* > 0$, and $D=D_{\max}$, where D^* is the value of D such that the homoclinic orbit of the positive constant steady-state intersects the v axis at $u=0$ (see Fig. 4). For this value of D there are only strictly positive nonconstant steady states on a finite interval (panels 2 of Figs. 6 and 7). Such remains the case for $D^* < D < D_{\max}$. A typical phase plane for $D^* < D < D_{\max}$ is shown in Fig. 5.

For $0 < D < D^*$ one may have all four types of periodic solutions. This is observable in Fig. 3, a typical phase plane for this case. The periodic orbit that touches the v axis at $u=0$ gives rise to the zero contact solution (panel 3 of Fig. 6). The orbits inside of this loop are smooth, positive, periodic solutions (panel 2 of Fig. 6) and orbits outside of this loop that start and finish on the v axis with $v \neq 0$ corresponds to nonzero contact angle solutions (panel 4 of Fig. 6). For each value of $D \in (0, D^*)$ there is a unique zero angle droplet solution. For $D \leq 0$ there are only the constant steady-state and nonzero contact angle solutions, see Fig. 2.

Similar remarks apply for spatially varying, steady-state solutions satisfying Neumann boundary conditions. For $D \leq 0$, nonzero contact angle droplets (orbits that begin and end on the v axis) and half-droplet (orbits that connect the u axis and v axis, panel 4 of Fig. 7) are possible. For $0 < D < D^*$, each of the solutions in Fig. 7 may arise (as well as full droplet versions). For $D \geq D^*$, nonconstant steady solutions must be strictly positive (panel 2 of Fig. 7).

V. NUMERICAL RESULTS

We have used a standard line search method (see, e.g., Ref. [18]) to solve the constrained minimization problem.

$$\text{Minimize: } F(\phi) = \int_0^L \left[\frac{\kappa}{2} |\phi_x|^2 + f(\phi) \right] dx.$$

$$\text{Subject to: } \text{Range}(\phi) \subset [0, 1] \text{ and } \int \phi dx = m.$$

A numerical solution to this problem with $L=1.0$, $m=0.5$ is shown in Fig. 8. This is a zero contact angle solution.

To consider full dynamics, we have used the numerical method presented in Ref. [19] to solve the initial value problem (7) with Neumann boundary and periodic boundary conditions. This is a finite element method that uses a subtle discretization of the nonlinearities which allows one to identify the discrete numerical flux with the flux in the continuous setting, which in turn allows one to establish positivity results for the discrete solutions. We remark that care must be taken to preserve the analytically proven positivity of the numerical solution and there are other choices for numerical method, see e.g., Ref. [20].

In all computations, we use

$$f(\phi_b) = \alpha \phi_b^3 (\phi_b/4 - \beta)$$

as the functional form of the homogeneous part of the cohesion energy density.

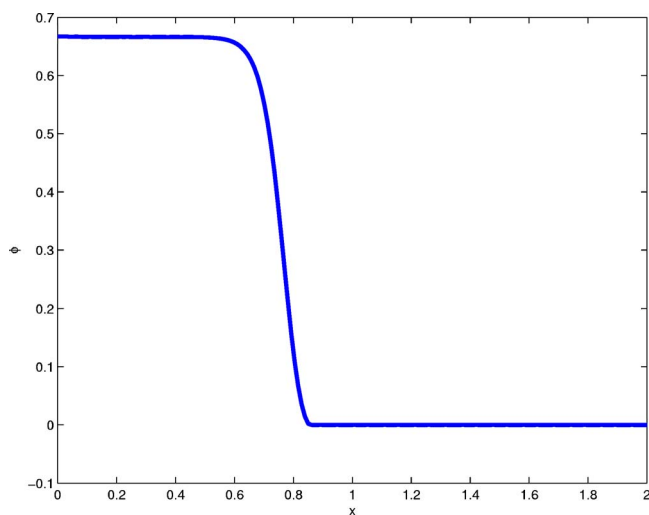


FIG. 8. (Color online) Solution of the constrained optimization problem of given mass 0.5.

A. Solutions with Neumann boundary conditions: Film formation

As it is possible for there to be different steady solutions with the same biomaterial mass, the question arises as to which is the most stable. In this regard, one can use the cohesion energy to ascertain which state is of lowest energy. It is known [15] that all strictly positive periodic solutions are saddles in the energy landscape with respect to zero-mean perturbations with periods longer than the period of the steady state. Similar results apply to steady states under Neumann boundary conditions. In particular, nonmonotone steady states are always unstable. We are unaware of theoretical results for the stability of monotone steady states. However, one would conjecture based on the results of Ref. [21] for the Cahn-Hilliard equation that it is possible to have stable monotone steady states.

We note that total biomaterial mass is conserved for the evolution equation (7) under periodic or Neumann boundary conditions. For a given fixed total mass, there is a one parameter family in D of monotone solutions. Varying D will result in variation of \hat{L} , the length of the support interval for the solution. In particular, \hat{L} increases with D . In Fig. 9, we have plotted one such family’s total energy as a function of \hat{L} for the total mass fixed at 0.5 with Neumann boundary conditions. The solution on the longest length interval is the zero contact angle solution (see the inset to Fig. 9). This solution also seems to be the solution of lowest energy out of the monotone solutions with fixed mass. Computations using full dynamics starting from perturbed, unstable, constant steady states also seem to tend to zero contact angle solutions (when such solutions are accessible), see, e.g., Fig. 10. We also note that this solution has the maximum possible value of D , i.e., minimizes $\int_0^L f'(\phi_b) dx$ among available steady solutions, see e.g., Fig. 11.

Thus we have the following observation: if the walls are sufficiently far apart (for a given, fixed biomaterial mass), then a uniform biofilm connecting the two walls will spontaneously “snap” and form a free surface (as in, for example,

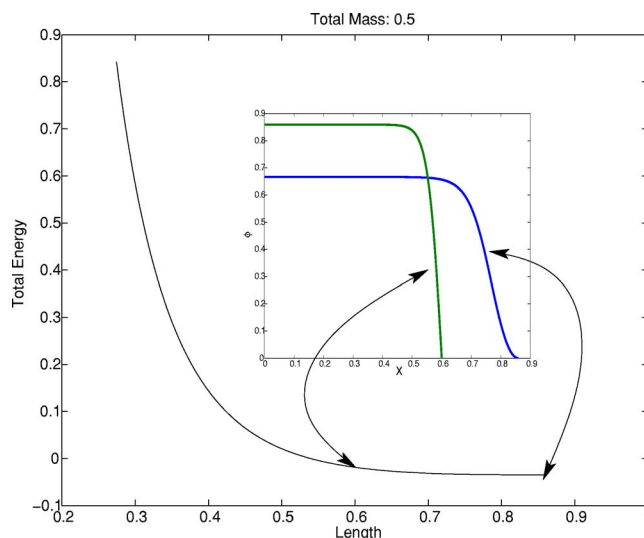


FIG. 9. (Color online) Energy plot for total mass 0.5. Inset: two solutions; the zero contact angle solution with minimum energy and a nonzero contact angle solution of higher energy. Both are of total mass 0.5.

Fig. 10). The form of the solution depends on both f and κ but minimizes $\int_0^L f'(\phi_b) dx$ (independent of κ). This is a principal result of this paper: cohesion energy results in a free surface biofilm.

B. Solutions with periodic boundary conditions: Nonhomogeneity

1. Breakup

Figure 12 shows the dynamic approach to a nonconstant, apparently steady solution starting from a perturbation of a constant solution. The results of Ref. [15] indicate though that this steady-state solution is in fact linearly unstable. Linearization of the discrete finite element approximation to the evolution equation (7) about this nearly steady state results in a large constant coefficient system of ordinary differential

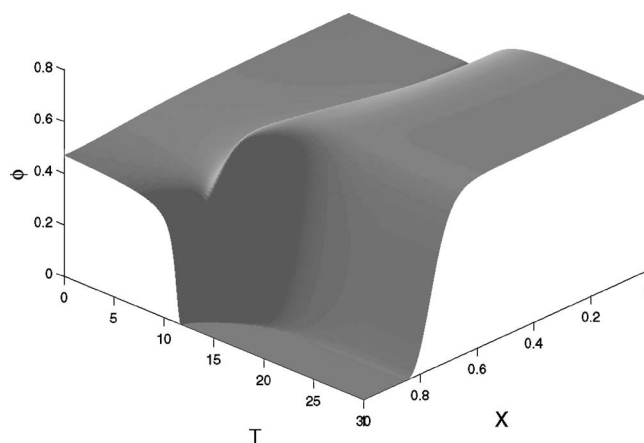


FIG. 10. Time evolution of a solution with mass per unit length 0.5 starting with a random perturbation of the constant solution, top view. The limiting solution appears to have zero contact angle.

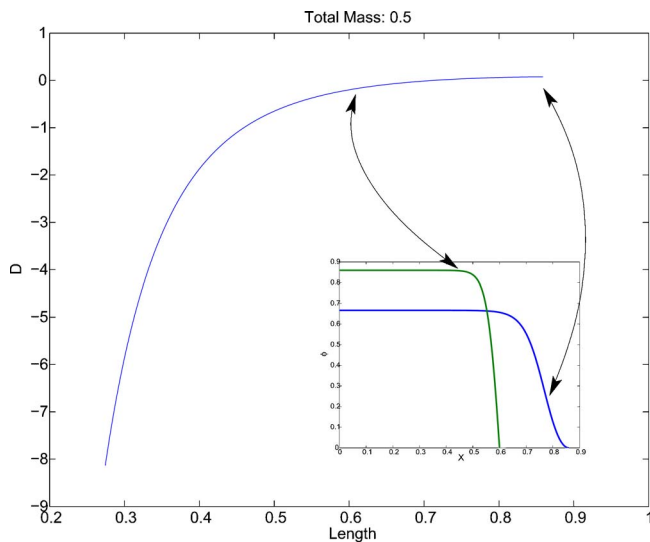


FIG. 11. (Color online) Plot of D vs L for total mass 0.5. Inset: two solutions; the zero contact angle solution with minimum energy and a nonzero contact angle solution of higher energy. Both are of total mass 0.5.

equations. We compute the eigenvalues of the matrix for the linear system using iterative techniques as in Ref. [22]. We have found numerically that the linearization matrix has positive eigenvalues of the order 10^{-7} . (A similar calculation for the single layer solution depicted in Fig. 8, however, yields all eigenvalues in the left-half complex-plane, indicating stability.) Thus, although in principle unstable, for the time scales of interest in the biofilm context we may be able to regard Fig. 12 as showing the approach to an almost steady, nonconstant, spatially periodic solution which for the purposes at hand may be regarded as stable.

In particular we note that solution breakup into droplets is possible. In the context of biofilms, break up may be interpreted to be a part of microcolony heterogeneity and channel formation (channels are widely observed voids within biofilms). Break up does not occur however where $D \geq D^*$. That is, when ϕ_b is sufficiently close to $\phi_{b,\text{infl}}$, break up does not occur. But this phenomenon may happen for smaller or larger values of ϕ_b , although it should be noted that spatially uniform solutions are energetically favorable for sufficiently

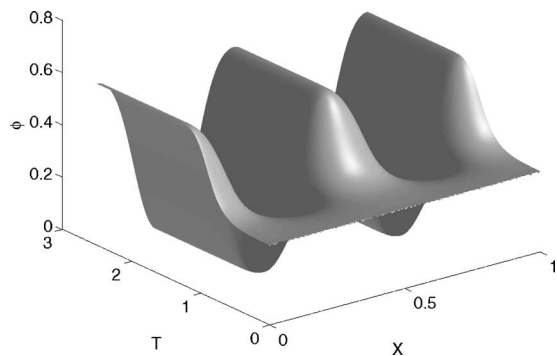


FIG. 12. Time evolution of a solution with total mass 0.3 starting with a random perturbation of the constant solution.

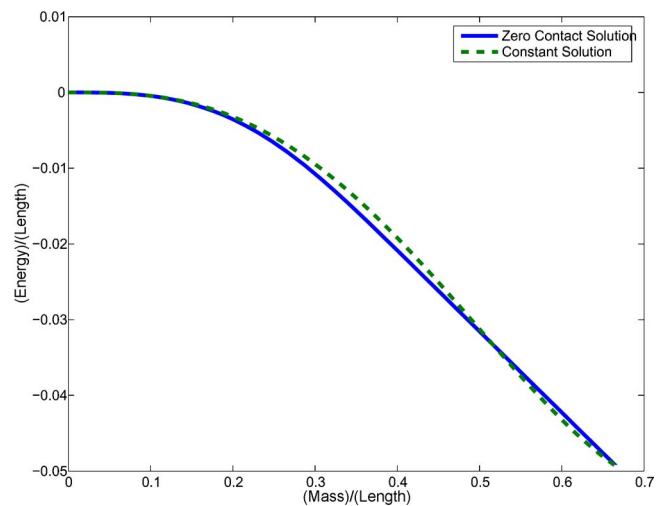


FIG. 13. (Color online) Energy plot for the zero contact angle solutions and the constant solutions.

large mass. We remark that internal heterogeneity in biofilms is frequently observed, see Ref. [23] for a quantification.

2. Bistability

As a remark, we note that the system (7) exhibits bistability. We have found numerically that it is possible to have a constant steady state and a nonconstant steady state, both linearly stable, for the same mass. Figure 13 shows an energy plot as a function of the mass per unit area. For this numerical study, f has $\phi_{b,\text{infl}}=0.5$ so that constant solutions are unstable for $\phi_b < 0.5$. We see in Fig. 13 that for smaller masses, zero contact angle droplet solutions are of lower energy than constant solutions, with a change-over in stability occurring as mass increases. However the change-over does not happen at the inflection point $\phi_{b,\text{infl}}=0.5$ (where the constant solution goes from being linearly unstable to being linearly stable) but slightly beyond. Hence in the small ϕ_b interval between inflection point 0.5 and actual energy crossover point, constant solutions are linearly stable but nonlinearly unstable. This situation is called nucleation instability in the polymer literature.

VI. DISCUSSION

We have derived equations describing biofilm mechanical behavior using a two component mixture of biomaterial and solvent. The main result of this paper is that minimization of cohesive energy results in spontaneous formation of free surface films, see, e.g., Fig. 10. Consequentially we argue that cohesion energy is fundamental to many aspects of biofilm mechanics. (For example, growth induced pressure stress is properly balanced by cohesion.) Further, in the presence of cohesion energy for sufficiently low density biomaterial, one-dimensional systems appear to spontaneously separate into microcolonies due to spinodal decomposition instability. In fact, full biofilm break up is possible, i.e., channel formation is observable. For higher density of biomaterial, but still smaller than the minimum energy density $\phi_{b,0}$, bistability is

observed with a heterogeneous state of lower energy than the homogeneous one. Thus nucleation instability is also possible. These mechanisms for inhomogeneity formation are the second observation of this paper, namely that internal inhomogeneities commonly seen in biofilms may at least in part be a consequences of cohesion. Of course there are other effects that may influence heterogeneity present as well, e.g., chemical signalling, diffusive transport limitations, etc. We do not discount their importance; our aim is merely to highlight a physical effect that has generally been overlooked in the biofilm community. As a remark, we note that these two observations, namely film formation and internal heterogeneity formation, arise out of the same linear instability, the spinodal decomposition. There are differences however in their nonlinear evolution due to boundary and far-field effects.

In order to focus on fundamental effects of cohesion, a number of important biological phenomena have been neglected including the impact of secretion and degradation of the extracellular polymer matrix and also the role of signalling molecules. Either of these may affect the form of the homogeneous cohesion energy density f as well as viscous

and elastic stresses. Perhaps of most immediate importance though, we have neglected biofilm growth and detachment, both of which may have effect on time scales comparable or shorter than that of cohesion. The interaction and balance of these aspects of biofilm development with cohesion may be of special interest in modeling as previous work has generally balanced growth in ad hoc ways. Other extensions of the two-phase model presented here may also be of interest; for example, it may be desirable to separate into three or more phases in order to describe different microbial species or to separate microbials from extracellular matrix.

To conclude, we argue that cohesion is an important physical effect that need generally be considered in a biofilm description. Relevance to failure and sloughing is obvious. But as results presented here suggest, long-time effects of cohesion may have biological importance also.

ACKNOWLEDGMENTS

This work was supported by NIH award Grant No. 5R01GM067245-02. The authors would like to thank A. Novick-Cohen for helpful comments.

-
- [1] J. W. Costerton, *J. Ind. Microbiol.* **15**, 137 (1995); P. Stoodley, K. Sauer, D. G. Davies, and J. W. Costerton, *Annu. Rev. Microbiol.* **56**, 187 (2002); J. W. Costerton and M. Wilson, *Biofilms* **1**, 1 (2004).
- [2] P. Stoodley, R. Cargo, C. J. Rupp, S. Wilson, and I. Klapper, *J. Ind. Microbiol. Biotechnol.* **29**, 361 (2002).
- [3] W. Gujer and O. Wanner, in *Biofilms*, edited by W. G. Characklis and K. C. Marshall (Wiley, New York, 1990), pp. 397–443; J. W. T. Wimpenny, in *Advances in Microbial Ecology*, Vol. 12 (International Society for Microbial Ecology, New York, 1992) p. 469; B. Rittman and J. Manem, *Biotechnol. Bioeng.* **39**, 913 (1992); C. Picioreanu, J. J. Heijnen, and M. C. M. van Loosdrecht, *ibid.* **58**, 101 (1998); S. W. Hermanowicz, *Math. Biosci.* **169**, 1 (2001); J. Dockery and I. Klapper, *SIAM J. Appl. Math.* **62**, 853 (2002); E. Alpkvist, N. Overgaard, S. Gustafsson, and A. Heyden, *Water Sci. Technol.* **49**, 187 (2004).
- [4] R. Dillon, L. Fauci, A. Fogelson, and D. Gaver, *J. Comput. Phys.* **129**, 57 (1996).
- [5] C. Picioreanu, M. C. M. van Loosdrecht, and J. J. Heijnen, *Biotechnol. Bioeng.* **72**, 205 (2001).
- [6] I. Klapper, C. J. Rupp, R. Cargo, B. Purvedorj, and P. Stoodley, *Biotechnol. Bioeng.* **80**, 289 (2002).
- [7] N. G. Cogan and J. P. Keener, *Math. Med. Biol.* **2**, 147 (2004).
- [8] E. Alpkvist and I. Klapper, *Bull. Math. Biol.* (to be published).
- [9] C. W. Wolgemuth, A. Mogilner, and G. Oster, *Eur. Biophys. J.* **33**, 146 (2004).
- [10] S. R. Lubkin and T. Jackson, *J. Biomech. Eng.* **124**, 237 (2002); H. M. Byrne, J. R. King, D. L. S. McElwain, and L. Preziosi, *Appl. Math. Lett.* **16**, 567 (2003).
- [11] S. T. Milner, *Phys. Rev. Lett.* **66**, 1477 (1991); M. Doi and A. Onuki, *J. Phys. II* **2**, 1631 (1992); H. Tanaka, *Phys. Rev. E* **56**, 4451 (1997).
- [12] T. Shaw, M. Winston, C. J. Rupp, I. Klapper, and P. Stoodley, *Phys. Rev. Lett.* **93**, 098102 (2004).
- [13] J. W. Cahn and J. E. Hilliard, *J. Chem. Phys.* **28**, 258 (1958).
- [14] Y. Jingxue, *J. Differ. Equations* **97**, 310 (1992).
- [15] R. Laugesen and M. Pugh, *Arch. Ration. Mech. Anal.* **154**, 3 (2000).
- [16] A. Ohashi, T. Koyama, K. Syutsubo, and H. Harada, *Water Sci. Technol.* **39**, 261 (1999); E. H. Poppele and R. M. Hozalski, *J. Microbiol. Methods* **55**, 607 (2003).
- [17] P. M. Chaikin and T. C. Lubensky, *Principles of Condensed Matter Physics* (Cambridge University Press, Cambridge, 1998).
- [18] D. Luenberger, *Linear and Nonlinear Programming* (Addison Wesley, Reading, MA, 1984).
- [19] G. Grün, *Math. Comput.* **72**, 1251 (2003).
- [20] J. W. Barrett, J. F. Blowey, and H. Garcke, *SIAM (Soc. Ind. Appl. Math.) J. Numer. Anal.* **37**, 286 (1999); L. Zhornitskaya and A. L. Bertozzi, *ibid.* **37**, 523 (2000).
- [21] M. Grinfeld and A. Novick-Cohen, *Trans. Am. Math. Soc.* **351**, 2375 (1999).
- [22] K. Meerbergen, A. Spence, and D. Roose, *BIT* **34**, 409 (1994).
- [23] K. Agladze, X. Wang, and T. Romeo, *J. Bacteriol.* **187**, 8237 (2005).